Journal of Chemical Health Risks

www.jchr.org

JCHR (2023) 13(3), 871-889 | ISSN:2251-6727

Development and Evaluation of PLGA Nanoparticles Loaded Allicin for Breast Cancer

Tarun Kumar[1], Dr. Vinay Pandit [2], Dr. Ranjit Singh[1]

[1]Adarsh Vijendra Institute of Pharmaceutical Sciences (AVIPS), Shobhit UniversityGangoh (UP)

[2]Professor & Head, Department of Pharmaceutics, Laureate Institute of Pharmacy Kathog (HP)

[3]Vice chancellor, Shobhit University Gangoh (UP)

(Received: 04 August 2023 Revised: 12 September Accepted: 06 October)

Graphical Abstract

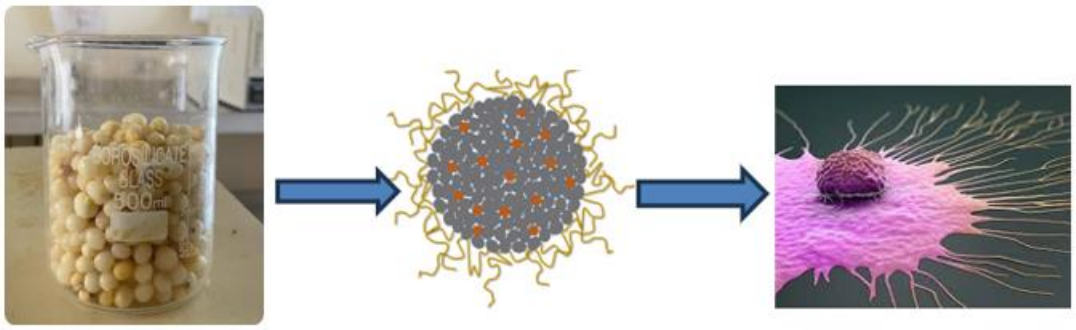

Allicin **Allicin-PLGA-NP** **Breast Cancer Cell**

KEYWORDS
Nanoparticles, PLGA, Allicin, breast cancer, design of experiment, target delivery

ABSTRACT:

The objective of this work was to design and develop Poly (D, L-Lactide-co-glycolide) (PLGA) Nanoparticles (NPs) of Allicin for treatment of breast cancer by Double Emulsification and Precipitation technique using stabilizer (poly vinyl alcohol). A systemic integration of design of experiment (DoE) based approach to design and to control process parameters yielded optimized final products. Three independent factors such as PLGA 50:50 (A), PVA (B), stirring speed (C) were considered. Three dependent responses were recorded in the experiment; Allicin release in 12th hour (Response 1), entrapment efficiency (Response 2) & particle size (Response 3). ATR and DSC studies indicated that there was no interaction between the drug and polymer. The morphological studies performed by SEM showed uniform and spherical shaped discrete particles without aggregation and smooth in surface morphology with a nano size range of 198.9 nm. X-ray diffraction was performed to reveal the crystalline nature of the drug after encapsulation. The NPs formed were spherical in shape with zeta potentials (4.4 mV). *In vitro* release studies were revealed drug release up to 12 hours. Allicin release kinetics study ascertained by First order kinetic study. Whereas release mechanism observed that, most of the formulations obeyed Higuchi. The cell viability was still more than 80% after incubation with the ALLICIN NP for 24 hours up to a concentration of 80 µg/ml. The Allicin NP carrier -treated MCF-7 display intrinsic cell damage and cell shrinkages compared with the control group. From the present investigation, it was concluded that PLGA NPs of Allicin may effectively deliver the drug and treats breast cancer.

Journal of Chemical Health Risks

www.jchr.org

JCHR (2023) 13(3), 871-889 | ISSN:2251-6727

Introduction

Herbal medicines involve plants or mixture of plant extracts to treat illness for promotion of health. [1, 2]. Over the past decades, in developing countries due to low economic rate and high cost of Western medicine, herbal medicine has an uninterrupted history of continuous usage by maximum population in the developing country, due to their cultural and spiritual points herbal medicines are more acceptable [3, 4].

Nanoparticles (NPs) are the particulate dispersions or solid particles drug carrier [5]. They have been generally used as a potential drug carrier for alternative of conventional drug release [6]. PLGA offers unique properties for drug delivery purposes like world-wide approval for medical use, biodegradability, biocompatibility, and controlled release. However, some issues are not manageable by a single polymer e.g. targeting the diseased tissue, cellular uptake together with pre-programmed intracellular trafficking, and escaping the reticuloendothelial system (RES) [7]. As the contact with the body and the consequences thereof are mediated via the surface of the device, surface modification of PLGA-particles by grafting with selected biomimetic ligands can meet some of these ambitious challenges to pave the way towards a more efficacious medication with reduced side effects and improved patient's compliance [8].

The Kashmiri garlic had been used from thousands of years to treat various types of disease. Botanical name of the plant is *Allium sativum* and is member of Alliaceae or Liliaceae family. It is used in various fields such as anti-cancer, anti-viral, anti-oxidant, and anti-inflammatory, anti-biotic, heart ailments, anti-acne, immunity booster, anti-diabetic, anti-obesity, and anti-arthritic [9,10]. Organic sulphur compounds in Kashmiri garlic are primarily responsible for its therapeutic properties. Allicin is the primary physiologically active compound in Kashmiri garlic [11,12].

The Kashmiri garlic plant's root bulbs were employed in all investigations. An Allicin concentration ranges from 1.61 percent to 13.03 percent of dry weight when Kashmiri garlic bulbs are crushed. Other portions of the Kashmiri garlic plant have received little research attention in terms of their chemical compositions and therapeutic benefits [13]. Therefore, in present work we aimed for the isolation and characterization of Allicin from Kashmiri garlic followed by its nanoparticulate formulation for the treatment of breast cancer.

Material and Methods

Materials

Poly(lactic-co-glycolic) Acid (PLGA) (50:50), ethyl acetate, and polyvinyl alcohol (PVA) were obtained from Sigma Aldrich Company, India. Fresh Kashmiri garlic bulbs were purchased from local producers in India. The human breast cancer cell line (MCF-7; ATCC HTB-22) was obtained from The American Type Culture Collection (ATCC). The cell culture growth medium was Dulbecco's modified Eagle's medium (DMEM; D5796) obtained from Sigma-Aldrich. The breast cancer cells were maintained in Dulbecco's Modified Eagle's Medium (DMEM) supplemented with 10% fetal bovine serum (FBS, 10499− 044; Gibco), 1% penicillin−streptomycin (P4333), and 1% amphotericin B (A2943) in 85% humidified atmosphere at 37°C and 5% CO_2. CytoTox 96 non-radioactive cell toxicity assay was obtained from Promega Corporation (Madison, WI, USA). All other reagents and chemicals used in the study were of analytical grade.

Extraction of Allicin from Kashmiri Garlic

The green Kashmiri garlic bulbs (mature garlic) were purchased from a local market in Kashmir, India. Prior to extraction, the dead auxiliaries were removed. The cleaned plants were separated into leaves, shoot and mature bulbs. The collected materials were washed in running tap water followed by rinsing in distilled water [14,15]. To extract the juice, 20 g of each material (collected from 10 plants) were crushed manually using a mortar and pestle, homogenized using a homogenizer (HeidolphSilentcrush M, Schwabach, Germany) and sonicated for 5 min continuously at 100% amplitude, using an ultrasonicator (UP200H, HielscherUltrasonics, Teltow, Germany) in 60 mL distilled water in an ice container. The obtained mash was squeezed through five layers of cheese cloth and the suspension transferred into 50 mL falcon tube and centrifuged (with Eppendorf 5810R) at 1500 rpm for 20 min at 4 ^{0}C in order to separate the remaining debris from liquid. The supernatant was transferred into a second sterile 50 mL falcon tube and sealed. The resultant extract was stored at 4 ^{0}C until use within 2 hr ensure the conversion of Allin to Allicin.

Journal of Chemical Health Risks

www.jchr.org

JCHR (2023) 13(3), 871-889 | ISSN:2251-6727

Above obtained fraction was subjected for Column chromatographic separation. A column made of borosilicate glass and measuring 30 cm in height was filled with silica gel and 10 gm of above fraction was placed into the column [16]. In gradient elution mode, the fraction was separated using mobile phase composed of methanol:water (50:50, v/v). The fraction obtained was subjected for TLC analysis using same mobile phase to check for the presence of single chemical component. TLC analysis revealed that there was presence of single spot indicating single component after visualization in iodine chamber.

Figure 1: Dried Isolated Fraction from Kashmiri garlic

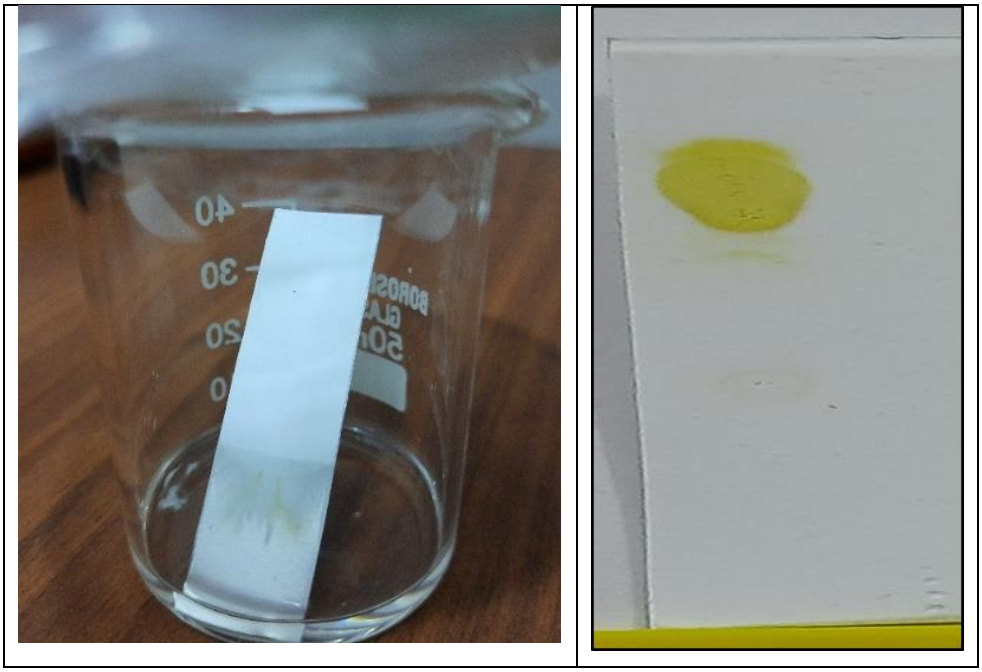

Figure 2: TLC analysis of obtained fraction

The obtained fraction from column chromatography was allowed for the evaporation and dried white powder was generated which was subjected for ^{1}H, ^{13}C NMR, and Mass analysis.100183-SND 400 MHz NMR instrument was used to generate ^{1}H, ^{13}C NMR graphs whereas LC-MS Shimadzu Mass instrument was used to get Mass spectra [17,18,19]. Tetramethylsilane (TMS) was used as internal standard in NMR analysis.

Molecular formula:$C_6H_{10}OS_2$; molecular weight: 262 gm/mol; R_f value: 0.92. Elemental analysis (*calc.*):C, 44.41; H, 6.21; O, 9.86; S, 39.52.

^{1}H NMR (400 MHz, DMSO-d_6, chemical shift (ppm)): δ3.219, 3.247, 3.308 (t, protons of carbon adjacent to sulfur atoms), 5.045, 5.098, 5.187, 5.201, 5.527, 5.576 (m, double bonded carbon protons), 5.902, 5.945, 5.965, 6.078, 6.187, 6.219 (m, double bonded carbon protons). The predicted and actual ^{1}H NMR spectrum along with structure are illustrated in Fig. 3

Journal of Chemical Health Risks

www.jchr.org

JCHR (2023) 13(3), 871-889 | ISSN:2251-6727

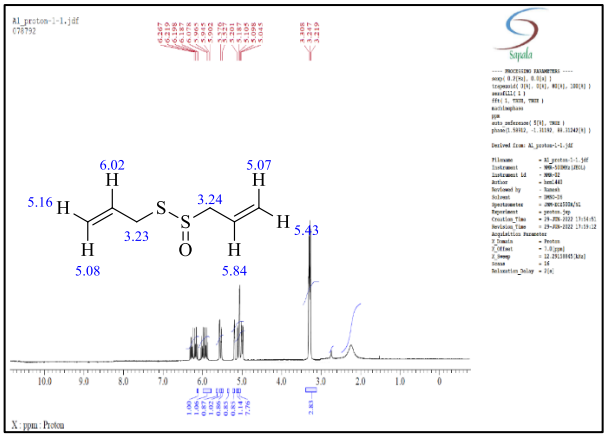

Figure 3: 1H NMR of isolated Allicin

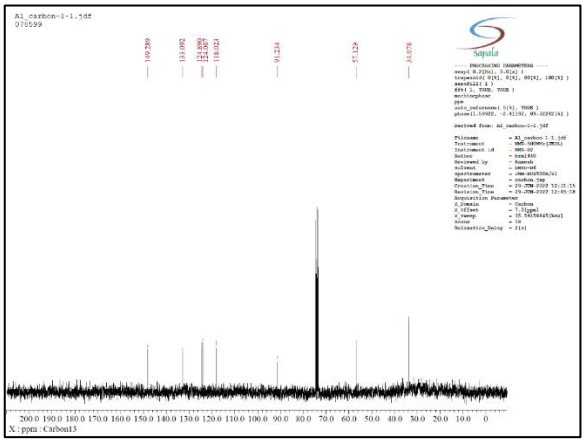

Figure 4: 13C NMR of isolated Allicin

^{13}C NMR (400 MHz, DMSO-d_6, chemical shift (ppm)):34.078, 57.129, 91.234, 118.023, 124.067, 124.890, 133.092, 149.289. Predicted and experimentally obtained ^{13}C NMRs of isolated compound are exemplified in Fig. 4 along with structure.

MS: m/z 262.67, 263.71 (m+1), 91.28 (fragment-1). The mass spectra of the compound is given in Fig. 5.

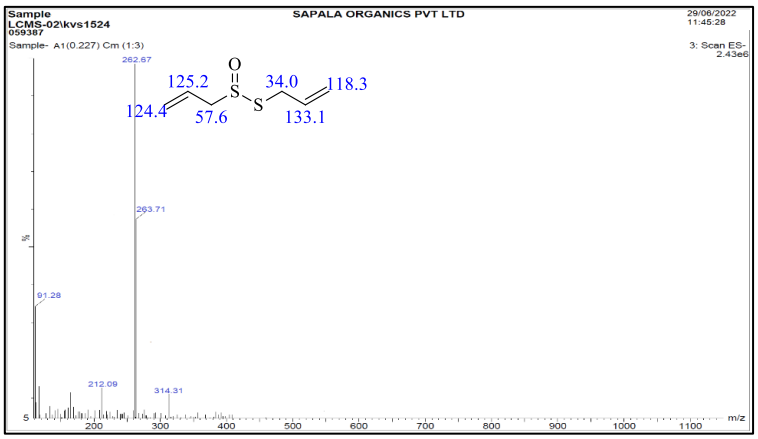

Figure 5: Mass Spectra of isolated Allicin

Characterization of Allicin Nanoparticle

Melting point (MP) determination

The capillary method involves placing the sample in a capillary tube and running an experiment that will heat the sample until it reaches melting point [20]. The melting point can then be recorded.

Solubility determination

The solubility of Allicin in various solvents such as 0.1 N HCl, Distilled water, Phosphate buffer 6.8, 7.4, Methanol, Ethanol and Dimethyl sulfoxide (DMSO) was determined by saturated solubility method. In this method excess of Allicin was added in a total of 2ml of each of the above-mentioned solvents and this solution was shaken on rotary flask shaker at room temperature for 24 hr [21,22]. The filtered supernatants were further diluted with solvent mentioned above and analyzed spectrophotometrically at 241 nm for their drug content. From these results, the solubility of Allicin in the respective solvent was calculated. All experiments were carried out in triplicate.

Preparation by Emulsification (Double emulsification) and Precipitation technique

Required quantity of Allicin was dissolved in a 1.0 ml of {DMSO: PEG (2%) solution}. In another beaker

Journal of Chemical Health Risks

www.jchr.org

JCHR (2023) 13(3), 871-889 | ISSN:2251-6727

specified amount of PLGA dissolved in 4 ml of DCM (Dichloromethane). The Allicin solution poured to PLGA solution which is precooled to 10°C and allowed for sonication in a probe sonicator (UAI-PS20khz-900W, Ultra Autosonic, India) for 10 minute at 6% amplitude. This procedure develops w/o emulsion. To that emulsion, specified amount of PVA (% w/v) solution was poured; covered with aluminium foil and further sonicated for 10 minutes under an ice bath to develop double emulsion [23,24]. Finally, 30 ml of PVA (1%) solution was added under magnetic stirring (1000 RPM, Remi stirrer, Mumbai, India) to evaporate excess DCM and DMSO. The precipitated nanosuspension was further washed with distilled water three times (Bench top centrifuger, Sigma 3-30 KS, Germany) for 15 minute to remove excess PVA by decantation. The resulted preparation lyophilized (BK FD10, Biobase, China) for 24h at -80°C and stored at 4°C for further evaluation and processing.

Formulations suggested by Box-behnken design (BBD)

A five-level three-factor Box-Behnken experimental design was used in the present study to evaluate the effects of selected independent variables on the responses. Three independent factors such as sodium PLGA 50:50 (A), PVA (B), stirring speed (C) considered (**Table 1**). The responses recorded in the experiment are Allicin release in 12th hour, EE, particle size. Mathematical fitting and analysis were performed by the *polynomial equation* [25,26]. The optimized formula was solved by graphical optimization technique along with a numerical method using the confidence interval value of alpha 0.05.

Table 1: Formulation Table

	Factor 1	Factor 2	Factor 3	Response 1	Response 2	Response 3	
Run	A:PLGA (50:50)	B:Poly vinyl alcohol	C:Stirring speed	EE	Particle size	% Allicin release at 12h	
	mg	%	RPM	%	nm	%	
1	250	2.5	3000	42	203	93.91	
2	150	2.5	4000	53	175	99.41	
3	250	3.5	2000	46	186	84.76	
4	350	2.5	2000	67	184	85.71	
5	150	2.5	2000	61	198	95.14	
6	150	3.5	3000	62	201	87.33	
7	350	1.5	3000	72	200	85.57	
8	250	2.5	3000	50	214	83.27	
9	250	2.5	3000	41	202	97.72	
10	250	3.5	4000	51	188	68.99	
11	250	2.5	3000	43	208	82.38	
12	250	2.5	3000	50	213	70.34	
13	150	1.5	3000	55	204	86.49	
14	350	3.5	3000	58	201	65.85	
15	350	2.5	4000	63	194	72.48	
16	250	1.5	4000	54	185	75.99	
17	250	1.5	2000	51	221	80.25	

Journal of Chemical Health Risks

www.jchr.org

JCHR (2023) 13(3), 871-889 | ISSN:2251-6727

Response surface methodology (RSM) is a collection of mathematical and statistical techniques for empirical model building [27]. By careful design of experiments, the objective is to optimize a response (output variable) which is influenced by several independent variables (input variables).

The study needs to validate the suitability of model selection as well as ANOVA analysis of independent variables with relation to Responses.

Characterization of Nanoparticles

In a 100 mL volumetric flask, an accurately weighed quantity of nanoparticles (Equivalent amount of 10 mg of Allicin) was placed, and the minimum amount of ethanol was added and thoroughly mixed. Approximately 10 minutes were spent sonicating (Ultrasonicator, CPX3800-E, Branson) the dispersion. Phosphate buffer with a pH of 6.8 was added to the resultant mixture and the volume was adjusted to the desired level [28]. The dispersion was bath sonicated for an additional 10 minutes, until it became transparent. The resulting mixture was subsequently filtered using a 0.45 m pore size Whatman membrane filter. To quantify Allicin content, the filtrate was analyzed with a UV-Visible spectrophotometer (Shimadzu UV-1800, Japan) at 241 nm.

Entrapment efficiency

$$EE\ (\%) = \frac{\text{Mass of Allicin in nanoparticle}}{\text{Initial mass of Allicin used in nanoparticle}} \times 100 \quad \text{.....(Equation 1)}$$

***In-vitro* Allicin release**

In vitro Allicin release from the nanoparticles was performed by diffusion technique using Franz-diffusion cell. The dialysis membrane; cellophane membrane was cut into equal pieces (6 cm×2.5 cm) and soaked into distilled water for 12 h before use [29,30]. The Allicin release studies of the solution is carried out in 10 ml of phosphate buffer pH 6.8 saline maintained at 37±0.5° with a magnetic stirrer with constant heating equipment (IKA Auto Temp Regulator, Germany). A sample of 2 ml of nanoparticles suspension was placed in receptor compartment. Aliquot samples of 1 ml were withdrawn at the regular interval and replaced with same volume of fresh buffer. The aliquots were diluted with fresh media, if necessary. Amount of Allicin diffused through the membrane was measured by using U.V. spectrophotometer at the wavelength 241 nm against phosphate buffer (pH 6.8) as the blank.

ATR study of Drug and Excipients

Attenuated total reflection (ATR) is a sampling technique used in conjunction with infrared spectroscopy which enables samples to be examined directly in the solid or liquid state without further preparation [31]. ATR spectroscopy is particularly useful for online monitoring of polymer composition. The study was conducted by ***ATR Bruker Opus 7.0, Germany.***

Differential Scanning Calorimetry (DSC) study

DSC is a thermal analysis apparatus measuring how physical properties of a sample change, along with temperature against time [32]. In other words, the device is a thermal analysis instrument that determines the temperature and heat flow associated with material transitions as a function of time and temperature. DSC was carried out by **DSC-60, Shimadzu, USA**.

X Ray Diffraction (XRD) study

X-Ray Diffraction, frequently abbreviated as XRD, is a non-destructive test method used to analyze the structure of crystalline materials and thereby reveal chemical composition information. XRD study was carried out by ARL EQUINOX 100, Thermo Scientific, India [33].

Surface morphology, Particle size and zeta potential of optimized formulation

Morphology of the prepared optimized Allicin nanoparticles was observed under scanning electron microscope. The sample was attached to the slab surface with double sided adhesive tape and the scanning electron microscope (S3700N-Hitachi, Japan) photomicrographs were taken at different magnifications [34]. Similarly, nanoparticles evaluated for particle size and polydispersity index value using the scattering light intensity technique (Malvern zetasizer, ATA scientific, USA)

Journal of Chemical Health Risks

www.jchr.org

JCHR (2023) 13(3), 871-889 | ISSN:2251-6727

Biological Studies

Cell Toxicity (LDH Assay)

The CytoTox96 assay kit was used to examine the cell-toxicity of ALLICIN NP carrier. LDH, a stable cytosolic enzyme produced during cell lysis, is quantified in the CytoTox96 assay. LDH is an enzyme that catalyses the inter conversion of pyruvate and lactate [35]. Fifty microliters of the control and test samples were put to a 96-well plate, along with the same amount of the LDH reagent, and the wells were incubated in the dark for 30 minutes at room temperature [36]. A multilabel counter (Perkin Elmer, VICTOR3 Multilabel Plate Reader, 1420) was used to measure the amount of LDH released spectrophotometrically at 490 nm.

Furthermore, the IC_{50} concentration was analyzed using the following equation

$$\text{Cell toxicity (\%)} = \frac{\text{OD of the experimental LDH release}}{\text{OD of the maximum LDH release}} \times 100$$

Cell Morphological Analysis

The cell morphology changes in 0 h- and 24 h-treated groups were visualized using a CKX41 inverted microscope (Olympus, Wirsam) connected to a camera with get IT software [37]. The cell morphology changes were captured at different time hours (0 and 24 h).

Results and Discussion

Melting point (MP) determination: The MP determined by G Lab Melting point was found to be 246.7°C

Solubility determination: High solubility was exhibited by organic solvent; maximum in DMSO followed by ethanol and methanol.

Table 2: Solubility of Allicin in different solvents

Solvent	Solubility (mg/ml)
0.1 N HCl	0.79±0.94
Distilled water	0.58±0.02
Phosphate buffer 6.8	0.62±0.04
Phosphate buffer 7.4	0.43±0.06
Methanol	3.07±1.72
Ethanol	3.28±2.64
DMSO	5.34±2.86

Optimization by BBD

Effect on independent variables on Response 1- % EE

The polynomial equation plotted and the synergistic and antagonist variables affecting the responses recorded.

Response 1 [EE]=45.2+**3.625A**-1.875B-0.5C-**5.25AB**+1.00AC +0.5 BC +**13.525A²** +3.025B² +2.275C² ……(2)

In Response 1, A, interaction term (AB) are significant.

Journal of Chemical Health Risks

www.jchr.org

JCHR (2023) 13(3), 871-889 | ISSN:2251-6727

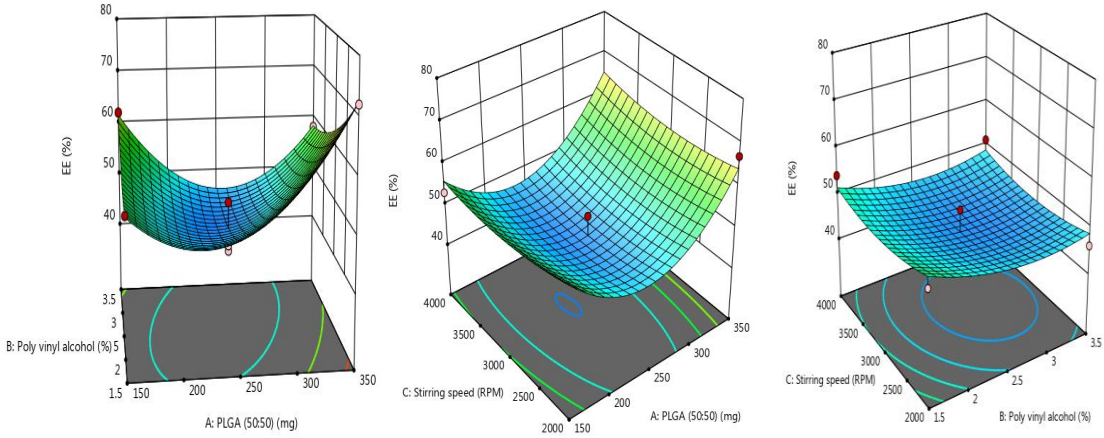

Figure 6: RSM curve of Response 1(EE)

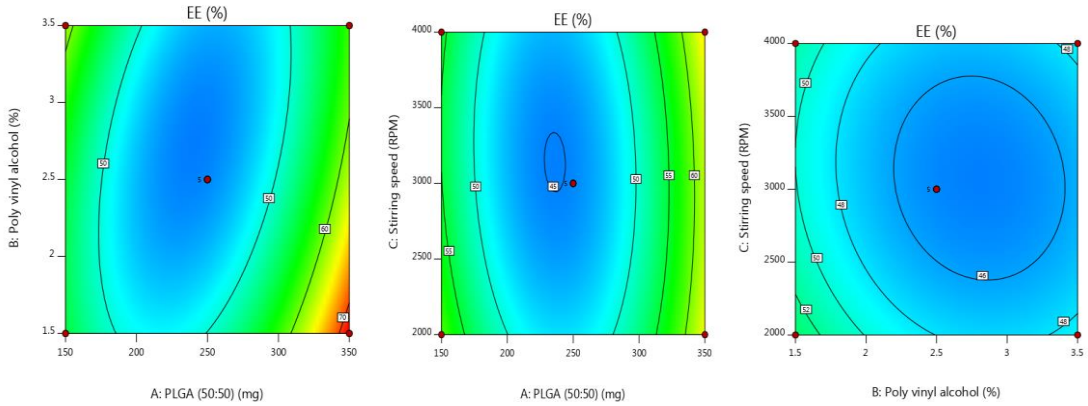

Figure 7: Contour plot of Response 1(EE)

Effect on independent variables on Response 2- Particle size

The polynomial equation plotted and the synergistic and antagonist variables affecting the responses recorded.

Response 2 [Particle size]= 208+0.125A-4.25B-**5.875C**+1.0AB+**8.25AC** +**9.5BC**-6.875A^2 +0.375B^2 -**13.375C^2**……..(3)

In Response 2, C, interaction term AC, BC, Quadratic term C^2 are significant.

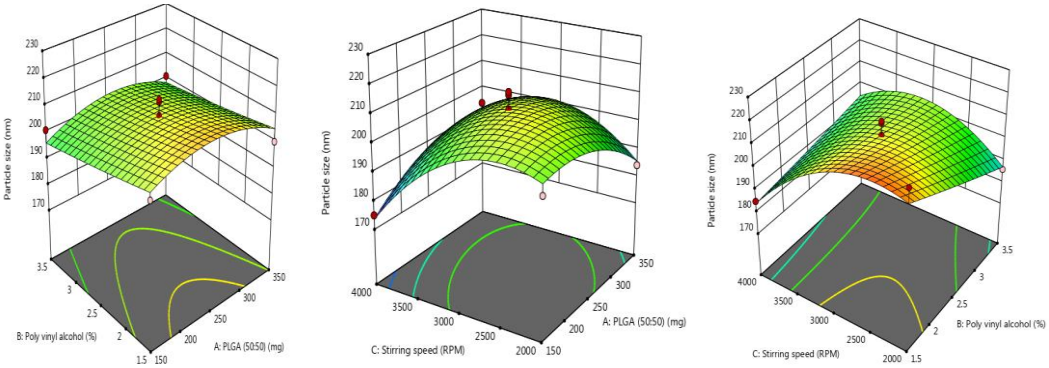

Figure 8: RSM curve of Response 2(Particle size)

Journal of Chemical Health Risks

www.jchr.org

JCHR (2023) 13(3), 871-889 | ISSN:2251-6727

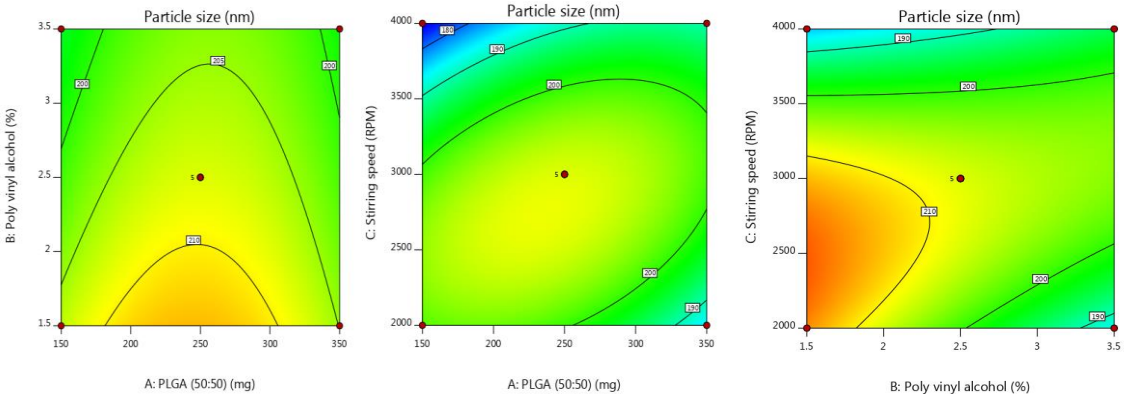

Figure 9: Contour plot of Response 2(Particle size)

Effect on independent variables on Response 3- % Allicin release at 12hr

The polynomial equation plotted and the synergistic and antagonist variables affecting the responses recorded.

Response 3 [% Allicin release at 12h]= 85.524-**7.345A**-2.67B-3.62C-5.14AB-4.37AC -2.87 BC + 3.23A^2-**7.45B^2**-0.57C^2……..(4)

In Response 3, A, C, Quadratic term (B^2) are significant

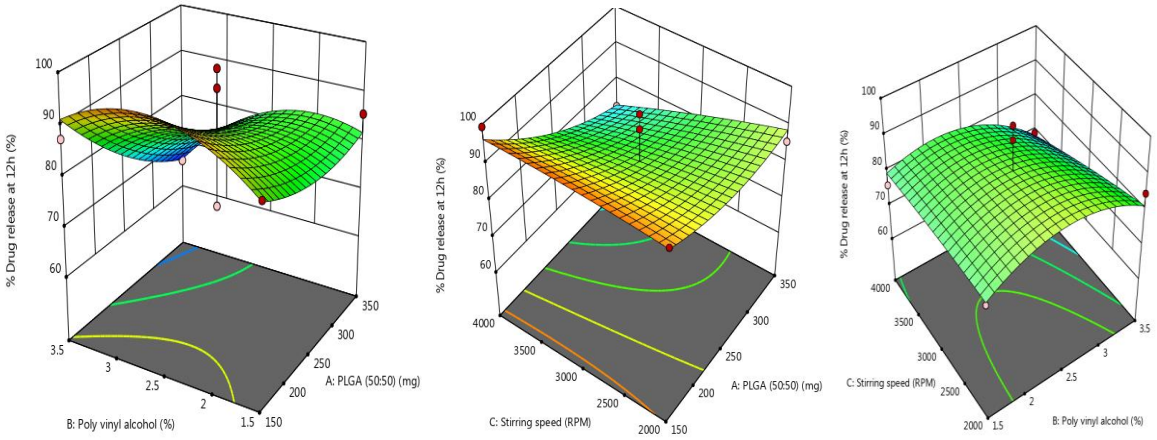

Figure 10: RSM curve of Response 3 (Allicin Release at 12 h)

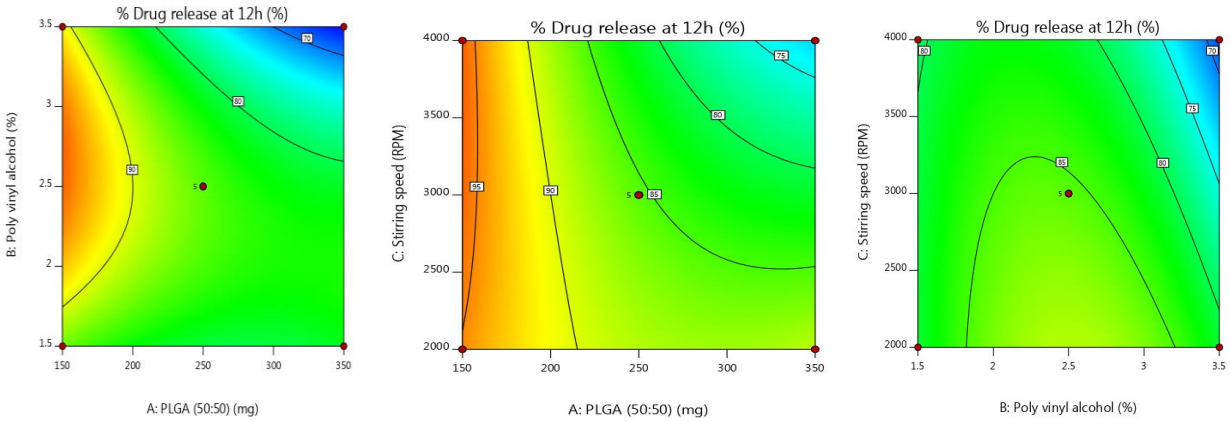

Figure 11: Contour plot of Response 3 (Allicin release at 12h)

Journal of Chemical Health Risks

www.jchr.org

JCHR (2023) 13(3), 871-889 | ISSN:2251-6727

Optimization of study

After generating the model polynomial equations, the process was optimized based on the relationship between the dependent and independent variables [38].

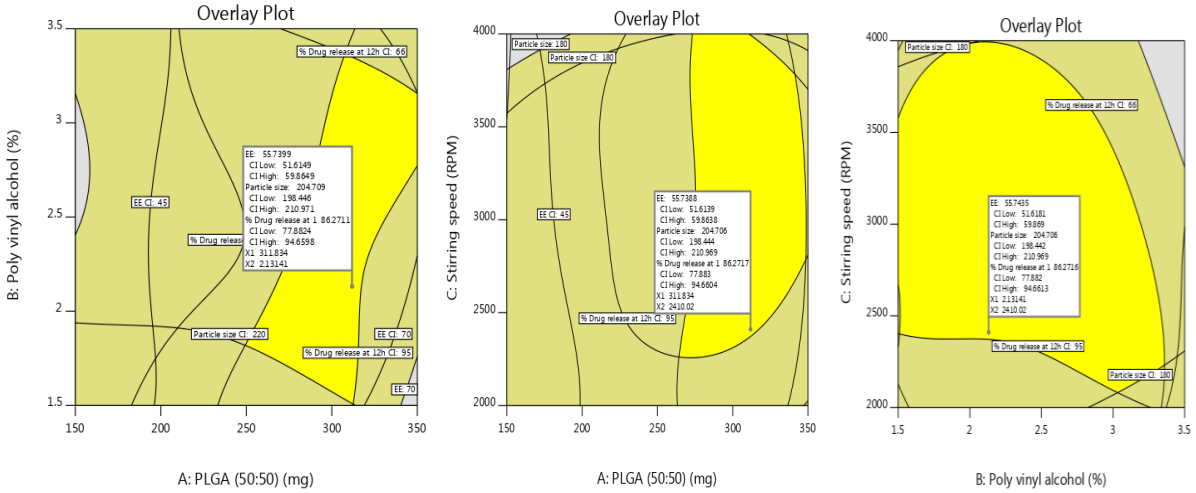

Figure 12: Overlay plot of region highlighting the optimized space and values

The final optimal experimental parameters were calculated using the canonical analysis. From the mathematical and graphical method of optimization; the best and optimized formulation developed and the design space (Yellow colour region) mentioned in Figure 12. Prior to the finding of optimized formulation, the target ranges (for responses) were fixed from the literature survey.

Table 3: Optimization formulation table

Factor	Name	Level	Low Level	High Level
A	PLGA (50:50)	324.79	150.00	350.00
B	Poly vinyl alcohol	2.18	1.50	3.50
C	Stirring speed	3703.04	2000.00	4000.00

Table 4: Point Prediction table of optimized formulation

Response	Predicted Mean	Predicted Median	Observed	Std Dev	SE Mean
EE	55.7421	55.7421	58.46	4.31029	2.17735
Particle size	204.705	204.705	168.9	6.54381	3.30562
% Allicin release at 12h	86.2715	86.2715	88.31	8.76555	4.42793

% EE

It was observed that, formulations loaded with high amount of PLGA (50:50) found high EE. Formulation "F7" have maximum 79.86%, F4 and F15 entrapped 72.46% and 69.26% respectively. Similarly, "F14" retained 64.67% of drug content. This clearly indicates hydrophobic nature of PLGA protected Allicin release from developed NPs. Similarly, the percentage amount of PVA signified the EE as it can be seen that 3.5% of PVA in F6 possessed highest EE whereas formulation (F13) with least amount of PVA i.e. 1.5% exhibited comparatively lesser EE of 60.48%. This could be due to high amount of PVA developed a viscous layer barrier which trapped more amount of Allicin in NPs. Finally, it can be concluded that, a suitable combination of PLGA and PVP can develop a NPs with good EE [39]

Journal of Chemical Health Risks

www.jchr.org

JCHR (2023) 13(3), 871-889 | ISSN:2251-6727

Table 5: Allicin loading of formulations F1-F17

Run	% EE	Run	% EE
F1	46.28	F10	55.12
F2	57.43	F11	47.66
F3	52.12	F12	54.03
F4	72.46	F13	60.48
F5	66.59	F14	64.67
F6	68.13	F15	69.26
F7	79.86	F16	58.11
F8	54.53	F17	57.27
F9	45.25	-	-

***In-vitro* Allicin release**

In vitro dissolution study of SLNs noted an appreciable amount of Allicin released in all formulation. But in "F4" it was found only 5% of Allicin released. The dissolution was carried upto 12, as few formulations released near to 100% release such as "F2"; released 99.41%, the highest. F4 released only 85.71%; whereas F5 released 95.14%. This indicated that, the higher amount of PLGA delayed Allicin release. A remarkable finding was also observed in formulations containing 350 mg of PLGA which is highest in composition as found in F4, F7, F14 and F15. It observed comparatively lesser Allicin release 85.71%, 85.57%, 65.85% and 72.48% respectively. This ascertained that, PLGA which is hydrophobic in nature, developed a barrier surrounding the NPs and hindered Allicin release.

Higher the amount of PVA developed a highly viscous layer and retarded drug release as compared to lesser PVA. The pattern can be seen in "F10" which released 68.99% however "F16" contributed 75.99% of Allicin. This above result conferred that both PLGA and high amount of PVA can contribute delayed drug release in suitable combination. While developing NPs stirring speed was also fixed as one of the independent variables. The RPM was fixed from 2000 as minimum and 4000 as highest value [40]. Higher RPM developed smaller NPs and lower RPM developed larger NPs as can be found in particle size analysis. F5 released 95.14% whereas F2 released 99.41% of Allicin in 12h. This ascertained the effect and contribution of RPM in dissolution pattern of NPs.

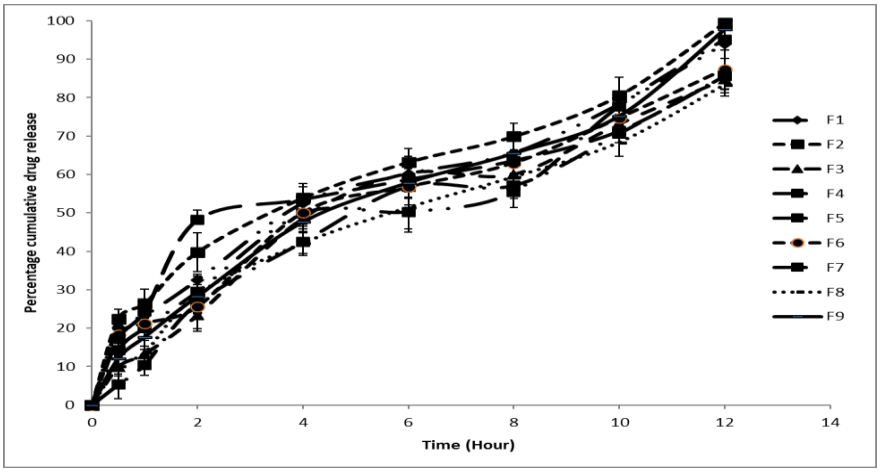

Figure 13: In vitro evaluation study of nanoparticles F1-F10

Journal of Chemical Health Risks

www.jchr.org

JCHR (2023) 13(3), 871-889 | ISSN:2251-6727

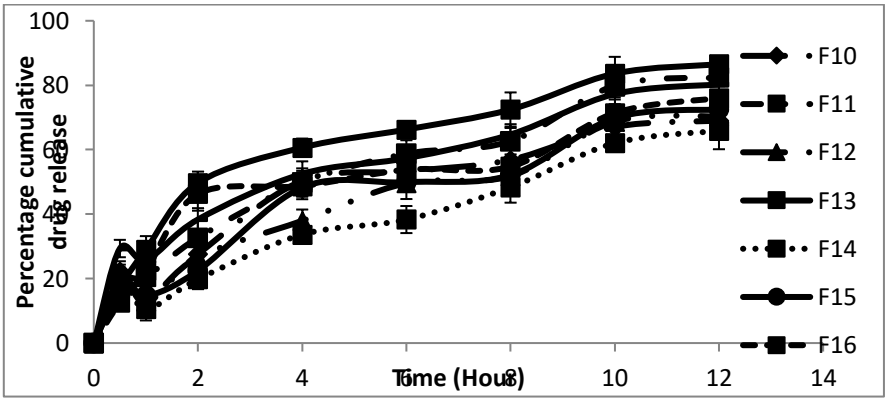

Figure 14: In vitro evaluation study of nanoparticles F11-F17

It was observed all formulation, first order R^2 value greater than zero order which indicate Allicin release primarily depend on Allicin concentration and polymer concentration. Whereas release mechanism observed for most of the formulations obeyed Higuchi. It is known that; Higuchi model describes the release of drugs from insoluble matrix as a square root of time dependent process. This data confers that, the high availability of PLGA in those formulations made hydrophobic nanoparticles and their release mechanism depended on surface area and change in diameter of the particle during the process of dissolution.

ATR study

Characteristic peaks were identified and characterized accordingly. The intense band in the region of 3274.06 cm^{-1} relative to OH groups, present only in the peel garlic extract spectrum, indicates that the ethanol used for its production was not completely removed. A characteristic broad peak appeared at 2122.65 cm^{-1} contributed by C-H stretching. Other important bands in this spectrum, are the one at 1637.98 cm^{-1} (C=O), and at 1390.63 cm^{-1} corresponding to organic compounds in containing sulfur. Other specific bands ascribed to sulfur also detected at 729.19 cm^{-1} (CS), 1042.48 cm^{-1} (S=O) and at 1138.76 cm^{-1} (SS).

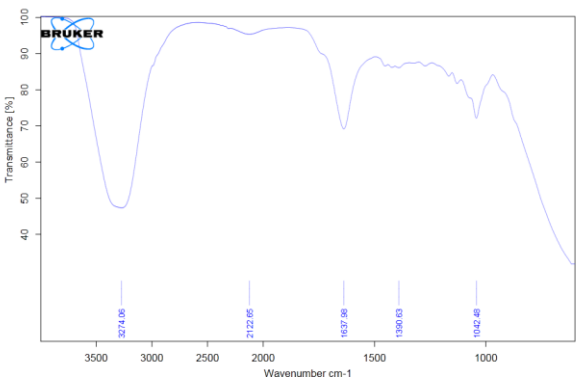

Figure 6. ATR spectra of Allicin

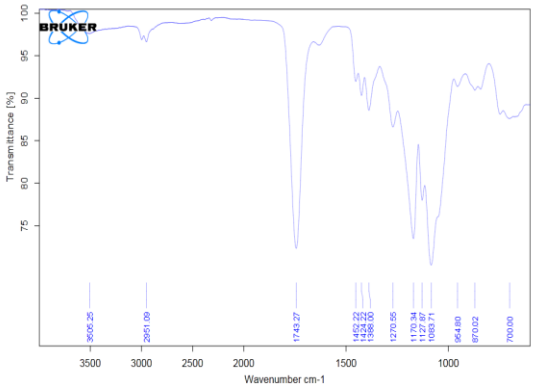

Figure 7. ATR spectra of Allicin + PLGA

Equal amount of drug and excipients taken in a clean and dry mortar pestle and triturated to get a physical mixture. The physical mixtures (Allicin + PLGA; Allicin + PVA) subjected to ATR study for compatibility determination.

It was observed that there are no such remarkable changes in peak position; which indicates compatibility of Allicin and other excipients.

Journal of Chemical Health Risks

www.jchr.org

JCHR (2023) 13(3), 871-889 | ISSN:2251-6727

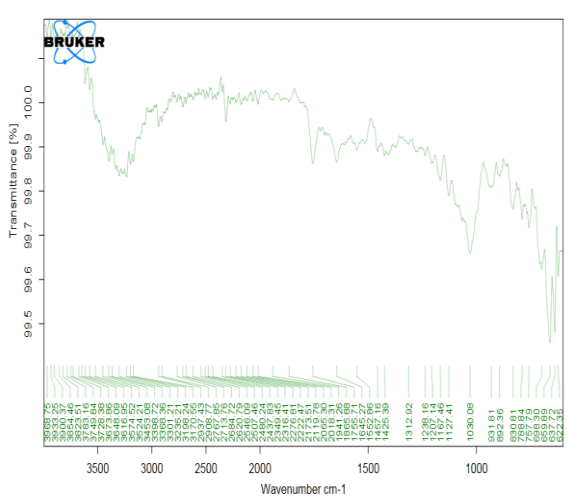

Figure 8. ATR spectra of Allicin + PVA

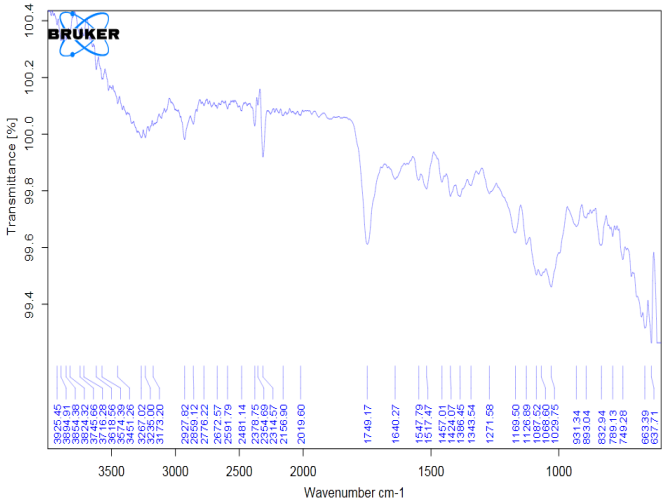

Figure 9: ATR spectra of optimized formulation

In optimized formulation, it was found that the intense band in the region of 3267.02 cm^{-1} relative to OH groups appeared, which was present in the peel garlic extract spectrum, indicated that the ethanol used for its production was not completely removed. Similarly, characteristic but weak peak appeared at 2156.90 cm^{-1} contributed by C-H stretching; this indicated formation of a weak interaction with co-excipient. However, an important band in this spectrum, at 1749.17 cm^{-1} attributed by C=O. Similarly at 1386.45 cm^{-1} corresponding to sulfur group found in optimized formulation. Similar to that pure Allicin, few other specific bands by sulfur also detected at 663.29 cm^{-1} (CS), 1029.75 cm^{-1} (S=O) and at 1126.89 cm^{-1} (SS). Finally, it revealed that, all the major groups related to Allicin found in optimized formulation and there was no such major interaction developed between Allicin and excipients.

Differential Scanning Calorimetry (DSC) study

A sharp endothermal peak at 104.18 °C with heat of energy of -18.02 mJ was observed; which is as per the literature study.

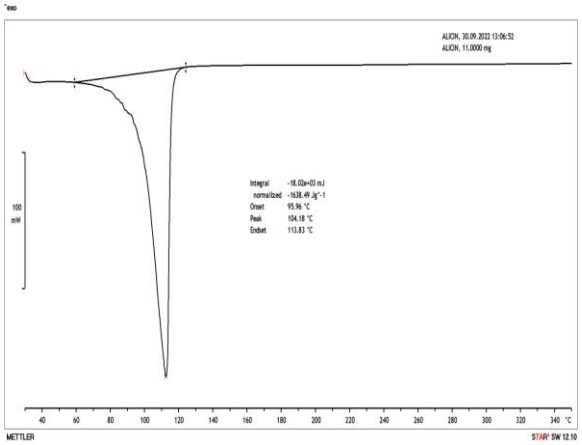

Figure 10: DSC of Allicin

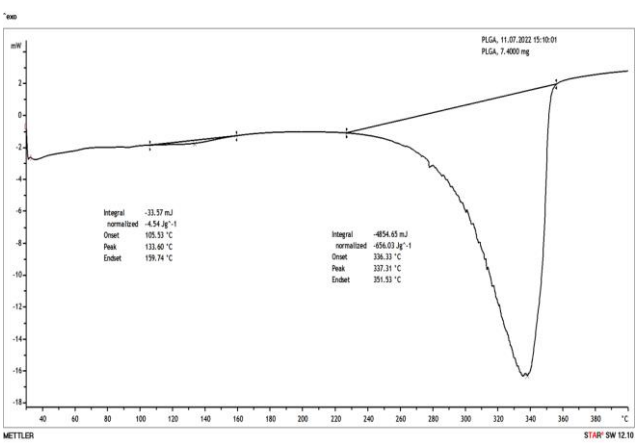

Figure 11: DSC thermogram of PLGA

PLGA exhibited characteristic peak at 337.31 which is as per literature review information provided.

Journal of Chemical Health Risks

www.jchr.org

JCHR (2023) 13(3), 871-889 | ISSN:2251-6727

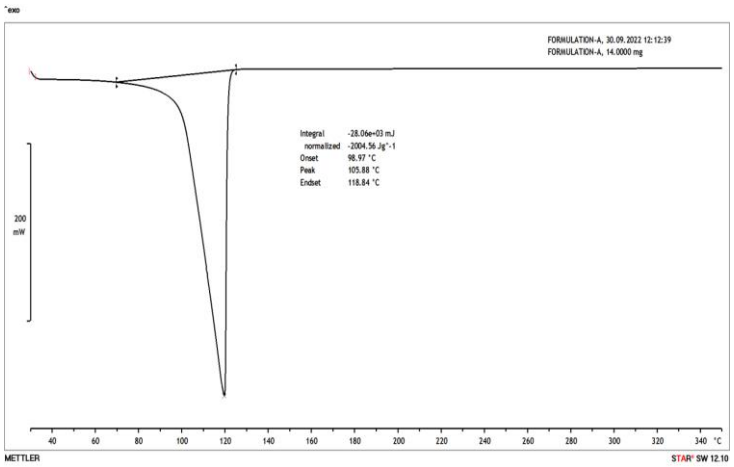

Figure 12: DSC thermogram of Optimized formulation

DSC study highlighted a sharp endothermal peak at 105.88 °C; which is near to pure Allicin as recorded earlier value of 104.18. This ascertained a no significant change in endothermal peak and indicated no-interaction with excipients considered in this study. However, it not observed the peak for PLGA (50:50); which need to be ascertained by further analytical technique.

X Ray Diffraction (XRD) study

While analyzing the information, a lot of noise was observed, which could be due to presence of moisture entrapped during the isolation of Allicin from crude extract. It noted a broad peaks at position 28 (2Theta) with intensity of 400. Few more characteristic peaks appeared at 42 (2Theta) and 63 (2Theta) with intensity below 400.

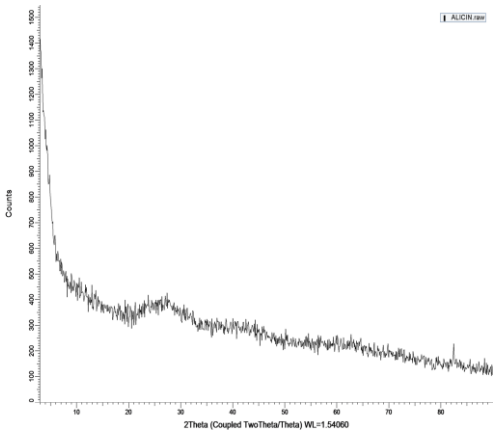

Figure 13: XRD of Allicin

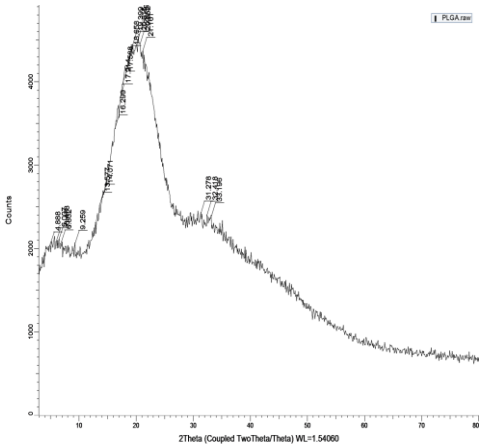

Figure 14: XRD spectra of PLGA

PLGA is considered in the current study as the primary polymer in the nanoparticles. During the XRD study, peak position (2Theta) and intensity was ascertained. A characteristic intense and broad peak at position 20.81 (2Theta) with intensity of 500. Few more additional peaks were also observed at 6.07 (2Theta) and 32.418 (2Theta) with intensity below 300.

XRD study highlighted significant characteristic peak at position 26.11 and 62.34 (2Theta) with intensity below 100, with few non-prominent peaks. A large number of small and minor peaks were appeared which could be due to presence of solvent and reduced crystallinity during formulation development.

Journal of Chemical Health Risks

www.jchr.org

JCHR (2023) 13(3), 871-889 | ISSN:2251-6727

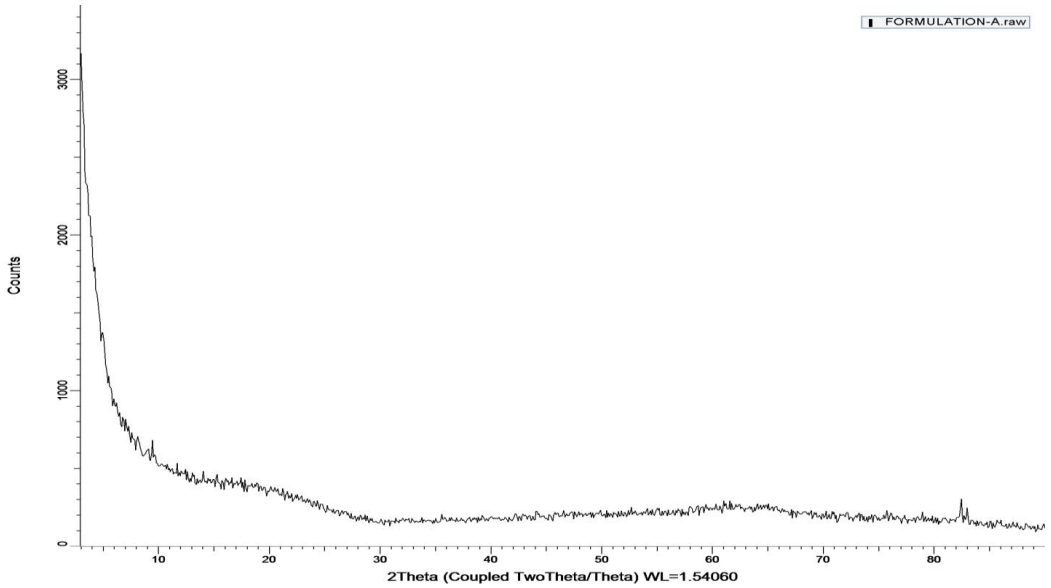

Figure 15: XRD spectra of optimized formulation

Surface morphology

Morphology of the prepared optimized Allicin nanoparticles was observed under scanning electron microscope.

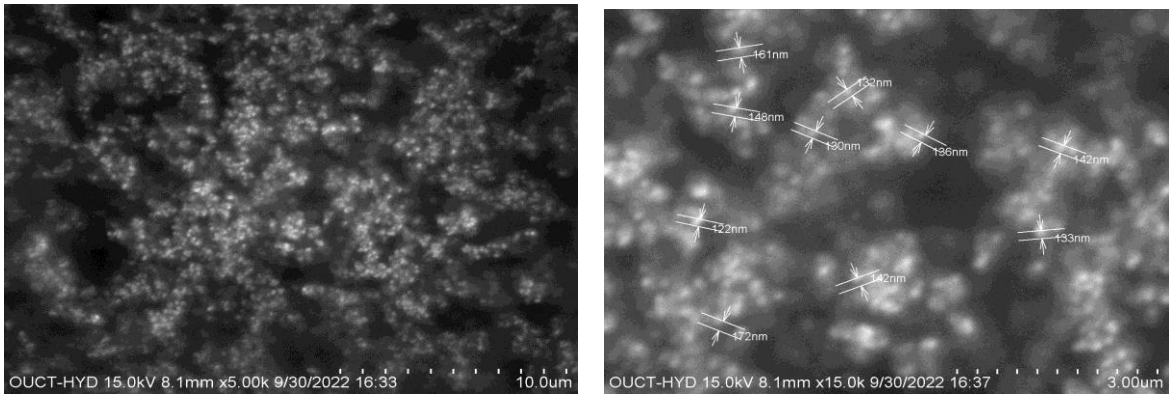

Figure 16: SEM study of Optimized formulation

SEM study revealed the appearances of optimized nanoparticles are spherical with smooth surface.

Particle size and Zeta potential

The particle size study revealed average size of 168.9 nm of optimized formulation. However, the data stated polydispersity index (PI) of 1.250 which indicated heterogenous dispersion.

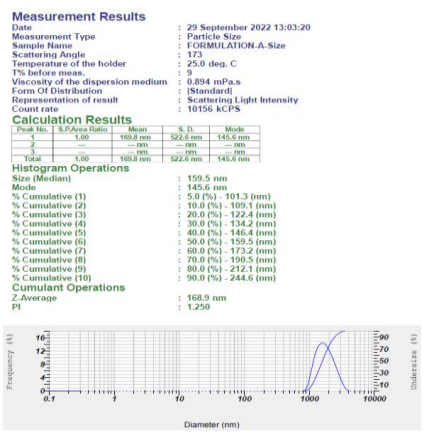

Journal of Chemical Health Risks

www.jchr.org

JCHR (2023) 13(3), 871-889 | ISSN:2251-6727

Figure 17: Particle size and distribution study of optimized formulation

Nanoparticles dispersed in acetate buffer pH 4.0 zeta potential were estimated. The study showed zeta value of 4.4 mV; indicated stability as per the literature available.

Measurement Results

Measurement Results

Date	: 29 September 2022 13:09:12
Measurement Type	: Zeta Potential
Sample Name	: FORMULATION-A-Zeta
Temperature of the holder	: 25.0 deg. C
Viscosity of the dispersion medium	: 0.894 mPa.s
Conductivity	: 1.114 mS/cm
Electrode Voltage	: 3.3 V

Calculation Results

Peak No.	Zeta Potential	Electrophoretic Mobility
1	4.4 mV	0.000034 cm2/Vs
2	--- mV	--- cm2/Vs
3	--- mV	--- cm2/Vs

Zeta Potential (Mean)	: 4.4 mV
Electrophoretic Mobility mean	: 0.000034 cm²/Vs

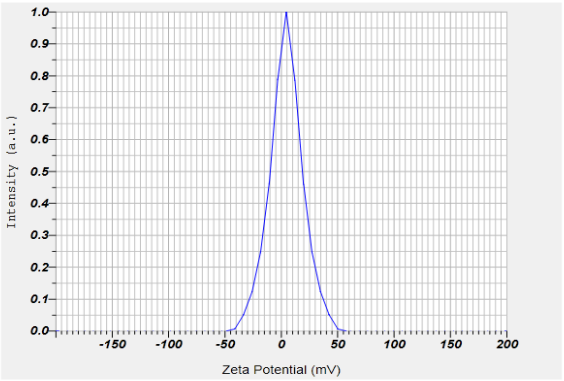

Figure 18: Zeta potential estimation of optimized formulation

***In-Vitro* Cell Toxicity (Lactate Dehydrogenase Assay)**

The cell-membrane damages of MCF-7 after treatment with different concentrations (1.25, 2.5, 5, 10, 20, 40, and 80 µg/ mL) of ALLICIN NP carriers were measured by the release of LDH using CytoTox96 assay. The percentage of toxicity gradually increased the concentration of as-prepared nanomaterials. The cell viability was still more than 80% after incubation with the ALLICIN NP for 24 h up to a concentration of 80 µg/ml. The higher cell toxicity effect of ALLICIN NP may be attributed to receptor-mediated endocytosis by MCF-7 cells, which increases the drug concentration in the intracellular environment.

Table 7: Concentration of drugs

	ALLICIN NP				
Conc. in mcg				**Mean**	**SD**
0	0	0	0	0	0
1.25	1.25	2.12	0.88	1.41	0.63
2.5	2	1.28	2.55	1.94	0.632
5	2.85	2.85	2.91	2.87	0.03
10	4	3.44	4.21	3.88	0.39
20	4.2	4.15	4.28	4.21	0.06
40	4.8	4.66	5.03	4.83	0.18
80	5.1	4.99	5.23	5.10	0.12

Journal of Chemical Health Risks

www.jchr.org

JCHR (2023) 13(3), 871-889 | ISSN:2251-6727

***In-Vitro* Morphological Analysis.**

In-vitro morphological changes of MCF-7 cells were observed by inverted light microscopy. There was an extreme morphology change in the MCF-7 cells after 24 hours of treatment. The Allicin NP carrier-treated MCF-7 displayed intrinsic cell damage and cell shrinkage compared with the control group.

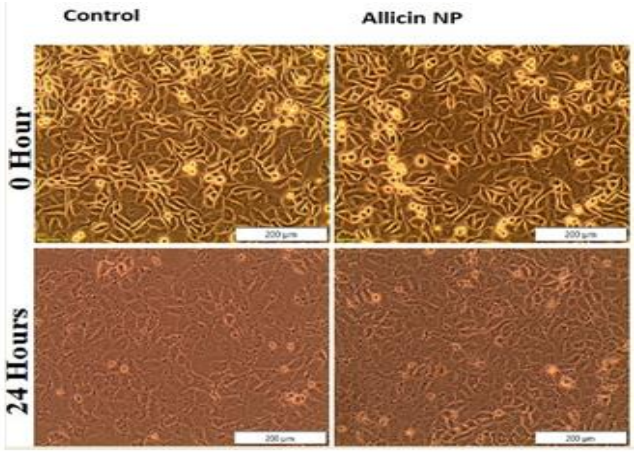

Fig 19: Invitro morphological changes

Conclusion

Allicin PLGA NPs were prepared by Double Emulsification and Precipitation Technique using design of experiment (DoE) based approach. Three independent factors such as PLGA 50:50 (A), PVA (B), stirring speed (C) were considered. Three dependent responses recorded in the experiment were Allicin release in 12th hour (Response 1), Entrapment Efficiency (Response 2), & particle size (Response 3). ATR and DSC studies indicated that there was no interaction between the drug and polymer. The morphological studies performed by SEM showed uniform and spherical shaped discrete particles without aggregation and smooth in surface morphology with a nano size range of 198.9 nm. X-ray diffraction studies were performed to reveal the crystalline nature of the drug after encapsulation. The NPs formed were spherical in shape with zeta potentials (4.4 mV). *In-vitro* release studies were discovered release up to 12 hrs. Allicin release kinetics studies ascertained by First order kinetic study and release mechanism was Higuchi. The cell viability was still more than 80% after incubation with the Allicin NP for 24 hours up to a concentration of 80 µg/ml. The present study concluded from the present investigation that PLGA NPs of Allicin may effectively deliver the drug and used in the treatment of breast cancer.

REFERENCES

1. Ossama M, Hathout RM, Attia DA, Mortada ND. Augmented cytotoxicity using the physical adsorption of Poloxamer 188 on allicin-loaded gelatin nanoparticles. The Journal of pharmacy and pharmacology. 2021;73(5):664-72.
2. Acharya, S., and Sahoo, S. K. (2011). PLGA nanoparticles containing various anticancer agents and tumour delivery by EPR effect. Adv. Drug Deliv. Rev. 63, 170–183. doi: 10.1016/j.addr.2010.10.008
3. Valko M, Leibfritz D, Moncol J, Cronin MT, Mazur M, Telser J. Free radicals and antioxidants in normal physiological functions and human disease. The international journal of biochemistry & cell biology. 2007;39(1):44-84.
4. Park S-Y, Cho S-J, Kwon H-c, Lee K-R, Rhee D-K, Pyo S. Caspase-independent cell death by allicin in human epithelial carcinoma cells: involvement of PKA. Cancer Letters. 2005;224(1):123-32.
5. Riley, R. S., and Day, E. S. (2017). Gold nanoparticle-mediated photothermal therapy: applications and opportunities for multimodal cancer treatment. Wiley Interdiscip. Rev. Nanomed. Nanobiotechnol. 9:e1449
6. Yao y, Zhou Y, Liu l, XU Y , Chen Q , Wang Y, Wu S, Deng Y, Zhang J and Shao A (2022). Nanoparticle –Based Drug Delivery In Cancer Therapy And Its Role In Overcoming Drug Resistance. *Front.Mol.Biosci*. 7:19
7. Monika Thakur, Roopali Sharma, Anand Kumar Mishra, Bandna Gupta, Body image disturbances among breast cancer survivors: A narrative review of prevalence and correlates, Cancer Research, Statistics, and Treatment, 10.4103/crst.crst_170_21, 5, 1, (90), (2022).
8. Smolarz B, Nowak AZ, Romanowicz H. Breast Cancer-Epidemiology, Classification, Pathogenesis and Treatment (Review of Literature). Cancers (Basel). 2022 May 23;14(10):2569.Bese NS, Munshi A, Budrukkar A, Elzawawy A, Perez CA. Breast ra-diation

Journal of Chemical Health Risks

www.jchr.org

JCHR (2023) 13(3), 871-889 | ISSN:2251-6727

therapy guideline implementation in low- and middle-income countries. Cancer. 2008;113(8 suppl):2305-2314.

9. Cazzaniga ME, Biganzoli L, Cortesi L, De Placido S, Donadio M, Fabi A, Ferro A, Generali D, Lorusso V, Milani A, Montagna E, Munzone E, Orlando L, Pizzuti L, Simoncini E, Zamagni C, Pappagallo GL. Treating advanced breast cancer with metronomic chemotherapy: what is known, what is new and what is the future?. *Onco Targets Ther*. 2019;12:2989-2997
10. Bahrami, B., Hojjat-Farsangi, M., Mohammadi, H., Anvari, E., Ghalamfarsa, G., Yousefi, M., et al. (2017). Nanoparticles and targeted drug delivery in cancer therapy. Immunol. Lett. 190, 64–83. doi: 10.1016/j.imlet.2017.07.015
11. Yang, Q., Jones, S. W., Parker, C. L., Zamboni, W. C., Bear, J. E., and Lai, S. K. (2014). Evading immune cell uptake and clearance requires PEG grafting at densities substantially exceeding the minimum for brush conformation. Mol. Pharm. 11, 1250–1258. doi: 10.1021/mp400703d
12. Zylberberg, C., and Matosevic, S. (2016). Pharmaceutical liposomal drug delivery: a review of new delivery systems and a look at the regulatory landscape. Drug Deliv. 23, 3319–3329. doi: 10.1080/10717544.2016.1177136
13. Chen, Y., Zhu, X., Zhang, X., Liu, B., and Huang, L. (2010). Nanoparticles modified with tumor-targeting scFv deliver siRNA and miRNA for cancer therapy. Mol. Ther. 18, 1650–1656. doi: 10.1038/mt.2010.136
14. Wang, X., Liu, X., Li, Y., Wang, P., Feng, X., Liu, Q., et al. (2017). Sensitivity to antitubulin chemotherapeutics is potentiated by a photoactivable nanoliposome. Biomaterials 141, 50–62. doi: 10.1016/j.biomaterials.2017.06. 034
15. Han, B., Yang, Y., Chen, J., Tang, H., Sun, Y., Zhang, Z., et al. (2020). Preparation, Characterization, and Pharmacokinetic Study of a Novel Long-Acting Targeted Paclitaxel Liposome with Antitumor Activity. Int. J. Nanomed. 15, 553–571. doi: 10.2147/ijn.s228715
16. Geisberg, C. A., and Sawyer, D. B. (2010). Mechanisms of anthracycline cardiotoxicity and strategies to decrease cardiac damage. Curr. Hypertens. Rep. 12, 404–410.
17. Eloy, J. O., Petrilli, R., Topan, J. F., Antonio, H. M. R., Barcellos, J. P. A., Chesca, D. L., et al. (2016). Co-loaded paclitaxel/rapamycin liposomes: development, characterization and in vitro and in vivo evaluation for breast cancer therapy. Colloids Surf. B Biointerfaces 141, 74–82.
18. Cagel, M., Tesan, F. C., Bernabeu, E., Salgueiro, M. J., Zubillaga, M. B., Moretton, M. A., et al. (2017). Polymeric mixed micelles as nanomedicines: achievements and perspectives. Eur. J. Pharm. Biopharm. 113, 211–228. doi: 10.1016/j.ejpb. 2016.12.019
19. Jiang, Y., Huo, S., Hardie, J., Liang, X. J., and Rotello, V. M. (2016). Progress and perspective of inorganic nanoparticle-based siRNA delivery systems. Expert. Opin. Drug Deliv. 13, 547–559. doi: 10.1517/17425247.2016.1134486
20. Cheng, C. A., Deng, T., Lin, F. C., Cai, Y., and Zink, J. I. (2019). Supramolecular Nanomachines as Stimuli-Responsive Gatekeepers on Mesoporous Silica Nanoparticles for Antibiotic and Cancer Drug Delivery. Theranostics 9, 3341– 3364. doi: 10.7150/thno.34576
21. Basoglu, H., Goncu, B., and Akbas, F. (2018). Magnetic nanoparticle-mediated gene therapy to induce Fas apoptosis pathway in breast cancer. Cancer Gene Ther 25, 141–147. doi: 10.1038/s41417-018-0017-2
22. Mandriota, G., Di Corato, R., Benedetti, M., De Castro, F., Fanizzi, F. P., and Rinaldi, R. (2019). Design and application of cisplatin-loaded magnetic nanoparticle clusters for smart chemotherapy. ACS Appl. Mater. Interfaces 11, 1864–1875. doi: 10.1021/acsami.8b18717
23. Mottaghitalab, F., Farokhi, M., Fatahi, Y., Atyabi, F., and Dinarvand, R. (2019). New insights into designing hybrid nanoparticles for lung cancer: diagnosis and treatment. J. Control Release 295, 250–267. doi: 10.1016/j.jconrel.2019.01.009
24. Colapicchioni, V., Palchetti, S., Pozzi, D., Marini, E. S., Riccioli, A., Ziparo, E., et al. (2015). Killing cancer cells using

nanotechnology: novel poly(I:C) loaded liposome-silica hybrid nanoparticles. J. Mater. Chem. B 3, 7408–7416. doi: 10.1039/c5tb01383f

25. Meng, H., Wang, M., Liu, H., Liu, X., Situ, A., Wu, B., et al. (2015). Use of a lipidcoated mesoporous silica nanoparticle platform for synergistic gemcitabine and paclitaxel delivery to human pancreatic cancer in mice. ACS Nano 9, 3540–3557. doi: 10.1021/acsnano.5b00510
26. Fang, R. H., Kroll, A. V., Gao, W., and Zhang, L. (2018). Cell Membrane Coating Nanotechnology. Adv. Mater. 30:e1706759. doi: 10.1002/adma.201706759 Farokhzad, O. C., and Langer, R. (2009). Impact of nanotechnology on drug delivery. ACS Nano 3, 16–20. doi: 10.1021/nn900002m
27. Maeda, H. (2001). The enhanced permeability and retention (EPR) effect in tumor vasculature: the key role of tumor-selective macromolecular drug targeting. Adv. Enzyme Regul. 41, 189–207. doi: 10.1016/s0065-2571(00)00013-3
28. Carita, A. C., Eloy, J. O., Chorilli, M., Lee, R. J., and Leonardi, G. R. (2018). Recent advances and perspectives in liposomes for cutaneous drug delivery. Curr. Med. Chem. 25, 606–635. doi: 10.2174/0929867324666171009120154
29. Sykes, E. A., Chen, J., Zheng, G., and Chan, W. C. (2014). Investigating the impact of nanoparticle size on active and passive tumor targeting efficiency. ACS Nano 8, 5696–5706. doi: 10.1021/nn500299p
30. Pelicano, H., Martin, D. S., Xu, R. H., and Huang, P. (2006). Glycolysis inhibition for anticancer treatment. Oncogene 25, 4633–4646. doi: 10.1038/sj.onc.1209597
31. Lim, E. K., Chung, B. H., and Chung, S. J. (2018). Recent advances in pH-sensitive polymeric nanoparticles for smart drug delivery in cancer therapy. Curr. Drug Targets 19, 300–317. doi: 10.2174/1389450117666160602202339
32. Jain, R. K. (1994). Barriers to drug delivery in solid tumors. Sci. Am. 271, 58–65. doi: 10.1038/scientificamerican0794-58
33. Shi, J., Xiao, Z., Kamaly, N., and Farokhzad, O. C. (2011). Self-assembled targeted nanoparticles: evolution of technologies and bench to bedside translation. ACC Chem. Res. 44, 1123–1134. doi: 10.1021/ar200054n
34. Farokhzad, O. C., and Langer, R. (2009). Impact of nanotechnology on drug delivery. ACS Nano 3, 16–20. doi: 10.1021/nn900002m
35. Danhier, F., Feron, O., and Préat, V. (2010). To exploit the tumor microenvironment: passive and active tumor targeting of nanocarriers for anti-cancer drug delivery. J. Control Release 148, 135–146. doi: 10.1016/j.jconrel.2010.08.027
36. H. Zhang, X.L. Liu, Y.F. Zhang, F. Gao, G.L. Li, Y. He, M.L. Peng, and H.M. Fan. Magnetic nanoparticles based cancer therapy: current status and applications. Science China Life Sciences 61: 400-14 (2018).
37. J. Peng, X. Liang. Progress in research on gold nanoparticles in cancer management. Medicine 98: 234-39 (2019).
38. Ales Sorf, Dimitrios Vagiannis, Fahda Ahmed, Jakub Hofman, Martina Ceckova, Dabrafenib inhibits ABCG2 and cytochrome P450 isoenzymes; potential implications for combination anticancer therapy, Toxicology and Applied Pharmacology, 10.1016/j.taap.2021.115797, 434, (115797), (2022).
39. H. Wang, X. Li, B.W. Tse, H. Yang, C.A. Thorling, Y. Liu, M. Touraud, J.B. Chouane, X. Liu, M.S. Roberts, and X. Liang. Indocyanine greenincorporating nanoparticles for cancer theranostics. Theranostics 8: 1227- (2018).
40. Pardeike, J., Hommoss, A., Müller, R.H. Lipid nanoparticles (SLN, NLC) in cosmetic and pharmaceutical dermal products. Int. J. Pharm. 2009, 366, 170–184.